J. Mountain Res. P-ISSN: 0974-3030, E-ISSN: 2582-5011 DOI: https://doi.org/10.51220/jmr.v20-i1.1
Vol. 20(1), (2025), 1-12

Green Synthesis of Biodegradable Cellulose Nanocrystals From Pine-Needles of *Pinus Roxburghii*

Aditi Kandari • Rita • Devendra Singh Negi*

Department of Chemistry, Hemvati Nandan Bahuguna Garhwal University (A Central University), Srinagar Garhwal, Uttarakhand-246174

*Corresponding Author Email Id: devendra_negi@yahoo.com

Received: 14.01.2025; Revised:18.02.2025; Accepted: 19.02.2025

Abstract: This study developed an eco-friendly method to synthesize cellulose nanocrystals (CNC) from *Pinus roxburghii* needles. Characterization techniques, including FTIR, SEM, DLS, TEM, AFM, XRD, TGA, and DSC, were used to assess the fabricated CNC. Mild chemical treatments enhanced the crystalline index from 60.6% to 82.7% by removing non-cellulosic and amorphous polysaccharides, as confirmed by XRD. FTIR analysis indicated successful cellulose isolation through characteristic peak shifts. AFM, TEM, SEM, and DLS revealed rod-like CNC with an average size of 179.4 nm. DSC analysis demonstrated CNC's high melting temperature and superior thermal stability compared to raw biomass, making them promising for nanotechnological applications.

Keywords: Cellulose • Cellulose nanocrystals (CNC) • Green synthesis • *Pinus roxburghii*

Introduction

The nanoscopic form of cellulose, known as nanocellulose has actuated extensive attention in current years towards the scientific society in the field of biomaterial sciences. Notably, cellulose can be found within almost all biomasses, including agricultural waste, forestry woods, bacteria, marine algae, tunicates, and many more (De Souza Lima & Borsali, 2004). In contrast to the bulk form of cellulose, nanocellulose preserves especially the biodegradable and regenerative properties of the cellulose, but besides that, it also has the advantages of biocompatibility, high degree of mechanical strength, massive surface area, low toxicity, low density, and extensive chemical modification owing to existence of rich hydroxyl groups and the great extent of hydrogen bonding networks(Michelin et al., 2020). Because of its distinct mechanical, chemical, optical, and rheological qualities, researchers have been interested in creating CNC from cellulose, which is renewable and widely available, over the past ten years (Balakrishan et al. 2018). Due to its exceptional properties and easy accessibility, nanocellulose is an emerging biodegradable polymer in the arena of nanotechnology and polymer industry. It also finds extensive application in the arena of food packing, textiles and paints, the pharmaceutical industry, optoelectronics, medical sciences, wastewater treatment, and drug delivery as well as in the environment protection field. (Thakur et al., 2021).

Structural morphology of nanocellulose: The primary module of the cell walls of plant is cellulose $(C_6H_{10}O_5)n$), which provides mechanical strength and stiffness to plants. Cellulose comprises a long chain of homo-polysaccharides or homoglycans with reiterating units of cellobiose ($C_{12}H_{22}O_{11}$) containing dualistic glucose molecules linked together with the formation of β-1,4 glycosidic linkage. β-D-glucose/glucopyranose of cellulose has $^4C_1$ chair conformation (Klemm et al., 2005). Several active -OH groups exist adjacent to cellulose backbone and occupy the

ring's equatorial position whereas H-atoms find their alignment at the axial position. Intra-molecular hydrogen bonding enhances the stability of this orientation of cellulose (Fig 1). $(C_6H_{10}O_5)n$ has a complex composition of β-D-glucose/glucopyranose which determines the kinetic chain length and grade of polymerization of nanocellulose-based material (Thakur et al., 2021) (Yadav, 2016)

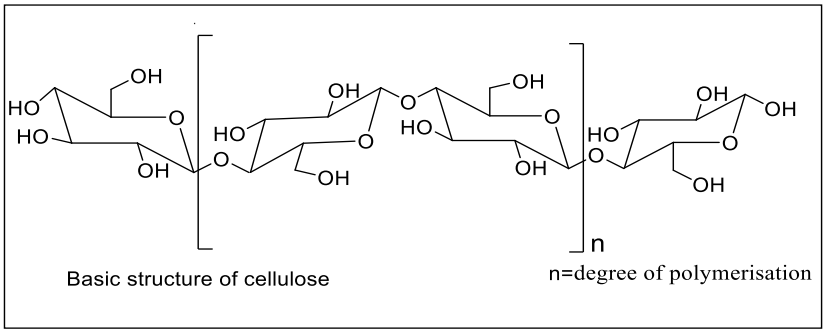

Fig. 1 Structure of cellulose.

Nanocellulose is divided into 3 major categories constructed on their synthesis circumstances:

1. (CNCs)cellulose nanocrystals, also raised to as cellulose whiskers,
2. (NFC) nano fibrillated cellulose or cellulose nanofibrils (CNFs),
3. Bacterial or electrospun cellulose(BC).(Nasir et al., 2017).

Acid hydrolysis of lignocellulosic biomass produces CNCs, having 3-35nm diameter along with 200-500nm length. In this process, most of the amorphous regions of nanocellulose are dissolved by concentrated acids, and rod-shaped CNCs with almost 90% crystallinity are left behind. In contrast to CNCs, both crystalline and amorphous regions are present in single strands of CNFs. They are extracted either by mechanical and chemical treatment or by arrangement of both treatments. These fibrils have a few micrometer length and a diameter of 5-100nm (Lin & Dufresne, 2014) . Bacterial cellulose is in ribbon shape that aggregates together to form a web-like structure with a diameter of 20-100nm. Bacteria such as Acetobacter , xylinum are used for the biosynthesis of BCs and this process involves the construction of small units (nm) from tiny units (Å). However, large-scale creation of bacterial cellulose is partial in comparison to CNFs and CNCs due to high expenses and low yield of BCs(Lee et al., 2014)Thus, the manufacture of CNFs and CNCs on an outsized scale is more favorable for practical applications.

Hence, keeping in mind the enormous potentiality of cellulose nanocrystals in various fields, in this piece of work we have targeted to extract the cellulose from needles of *Pinus roxburghii* which are abundant in India's Himalayan areas. Each summer, the forest's needles catch fire, causing a significant loss of plants and animals as well as eventual pollution and energy consumption (Thakur et al. 2013). According to the literary texts, between 1.37 and 2.37 million tonnes of *P. roxburghii* needles is available annually in Uttarakhand, India (Kala & Subbarao 2018). However, using these needles as fibers will help reduce the significant loss of forests by using easily accessible needles to create cellulose nano crystal, an environmentally benign biopolymer. With minimal expense and gentle chemical processing, CNC has been produced from the easily accessible and affordable material. Because of the increased surface area, crystalline structure, and amount of accessible functional groups, the conversion of cellulose to CNC is more efficient. Several experimental techniques, including XRD, FTIR, TEM, AFM, SEM, DLS, and DSC,

provide a good description of the CNC that was created.

Materials and Methods

Pinus roxburghii needles were acquired from forest area of Pokhal, Tehri Garhwal, Uttarakhand (Fig 2). This area is recognized for its biodiversity and renewable plant resources. The choice of *P. roxburghii* as the raw material on behalf of CNC extraction was determined by its availability, simplicity of collection, and appropriateness for conversion into cellulose-based products. Chemicals including ethanol, sodium hydroxide (NaOH), sodium hypochlorite ($NaClO_2$), and sulfuric acid (H_2SO_4), are of analytical grade obtained from Fisher Scientific.

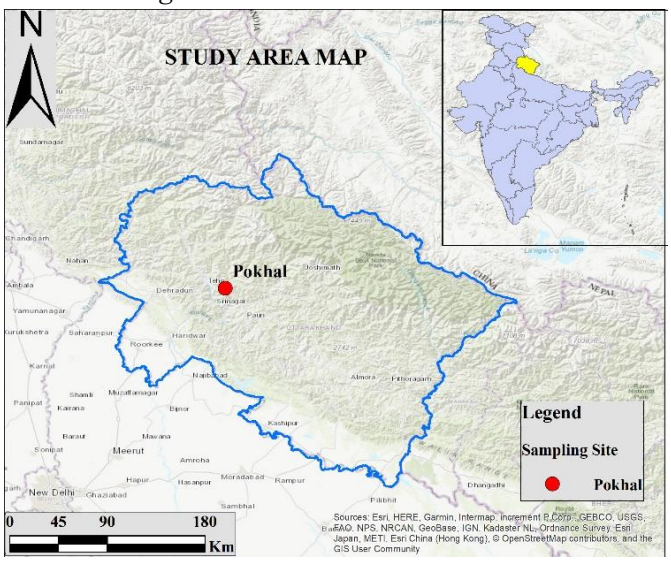

Fig. 2 Study Area.

Refining and extraction of cellulose

Pinus roxburghii needles were dried and grinded into powder. Cellulose was extracted using slightly modified versions of previously reported procedures (Azizi et al. 2014; Kalia et al. 2011; Kumar et al. 2014; Khalil et al. 2014; Ng et al. 2015; Johar et al. 2012). To eliminate phenolic compounds, wax, and pigments, the dried powder (20 g) was extracted using Soxhlet in ethanolic solvent.

Following dewaxing, the resulting biomass was subjected to alkaline treatment with 5 % NaOH solution while maintaining steady agitation for 6 hours at 80 ° C . The residual brownish product, including lignin and cellulose, was washed with distilled water until the pH was neutral. Following this treatment, the resultant fibers were bleached thrice by 1.5% $NaClO_2$ solution at 50 °C for eight hours. The procedure was improved by using a few drops of acetic acid while maintaining continuous mechanical stirring for 8 hours at 50 ° C. The bleached fibers were flushed thoroughly with distilled water to attain the neutral pH, and finally white aqueous solution was ultimately freeze-dried to get white-colored pure cellulose.

Preparation of CNC

To obtain CNCs, cellulose from pine needles were acid hydrolyzed by 30% aqueous H_2SO_4 solution for 6 h at 50 ° C by constant stirring. The resulting suspension was then diluted through ice cold water to halt the acid hydrolysis reaction. Further, it was centrifuged at 10,000 rpm for 10 minutes in order to precipitate the CNC and eliminate extra aqueous acid. The process was repeated 4 times, with the precipitated material being washed thoroughly with distilled water . The residual CNC suspension was dialysed in contradiction of deionized water until the suspension obtained a constant pH and finally, the subsequent material was freeze dried to

achieve cellulose nanocrystals (Gibril et al. 2022).

Characterization techniques

Physico-chemical characterization: The **FTIR** spectra of the raw fiber, extracted cellulose, along with synthesized cellulose nanocrystal, were obtained at a wavenumber between 4000 and 500 cm^{-1} at a resolve of 4 cm^{-1} with four scans per sample. After being oven-dried at 105 ° C for 5 hours , samples were joint through KBr in a 1:200 (w/w) ratio and creased under vacuum to make pellets. The transmittance mode was used to record the FTIR spectrum of samples (Kumar et al. 2014).

Measurements of **XRD** were carried out to determine the crystallinity index of samples at a scanning velocity of 0.02° per second, diffraction patterns existed acquired throughout a 2θ range of 10° to 80° (French 2014). The following formula mentioned by Nam et al. (2016) be present used to conclude crystallinity index (CrI %) of cellulose in the CNC and CNC/ZnO composite:

$$\text{CrI (\%)} = \frac{I020 - Iam}{I020} * 100$$

Where, I_{am} is the diffraction intensity in the valley between peaks (101) and (002) ascribed to amorphous cellulose and I_{020} is the extreme spreading intensity of the distinctive peak (002) at about 22-23°.

Morphology, size distribution and surface charge: SEM was used to inspect the morphological configuration of grounded needles of *Pinus roxburghii* both before and after chemical treatments. An Agar Sputter Coater was used to apply a thin layer of gold-palladium in an argon environment to samples that had been placed on carbon tapes. The electron micrographs were captured utilizing secondary electrons and a multi-segment BSED finder in a high vacuum mode with an acceleration voltage of 15 kV (Rambabu et al. 2016).

For **TEM**, a small drop of a diluted aqueous suspension (0.05 weight %) was applied on the external of a copper grid covered by a thin layer of carbon. The samples were dried preceding TEM investigation, which was approved out by an accelerating voltage of 100–120 kV (Fardioui et al. 2016). An **AFM** was a charity to twin the morphology and topography of the CNC and nanocomposite. A droplet of the aqueous suspension was first dry on a glass slide, and then the images were taken in the air in a semi-contact mode (Fardioui et al. 2016). The hydrodynamic size and the zeta potential were determined with the aid of DLS analysis. For this, the samples were deferred in deionized water, and exposed to ultrasonication for homogeneity (Babick 2020).

Thermal analysis: DSC measurements were conducted by using 5 mg of sample in a sealed aluminium pan at a rate of 10 °C/min as of 30 to 600 °C in a nitrogen environment thru a flow rate of 30 mL/minute (Leyva-Porras et al. 2019).

Results and Discussions

Isolation of cellulose and synthesis of CNC: The raw pine needles and their powdered form were brown in color, as given in Figure 3(a and b). As a result of dewaxing, alkali, and bleaching the cellulose was extracted, and the fiber's texture, and color of raw biomass changed to white (Figure 3c). The elimination of certain functional groups, which were visible in the FTIR data is an indicator of extraction of pure cellulose and removal of non-cellulosic components. Whiter (Figure 3d) and finer-textured CNC was obtained by hydrolyzing the isolated cellulose with H_2SO_4 followed by washing of product until neutral pH was attained. The clear gel produced, was under-processed by cold centrifugation (at 10,000 rpm). The subsequent white CNC powder was obtained by freeze-drying the gel for 24 hours (Fig. 3e).

Fig. 3: Physical aspect of the (a) raw dried pinus needles (b) Grinded pinus needles (c) Extracted cellulose (d) Nanocellulose suspension (e) Cellulose nanocrystal powder

Characterization analysis

Physico-chemical characterization: The FTIR spectra of the raw pine needles, delignified pine needle, extracted cellulose, and pine needle synthesized nanocellulose are revealed in Fig. 4. In all the samples a faint peak at 2900 cm^{-1} and a broad intense peak at 3450 cm^{-1} is displayed due to the distending vibrations of C-H groups and O-H groups of cellulose (Mandal and Chakrabarty 2011).

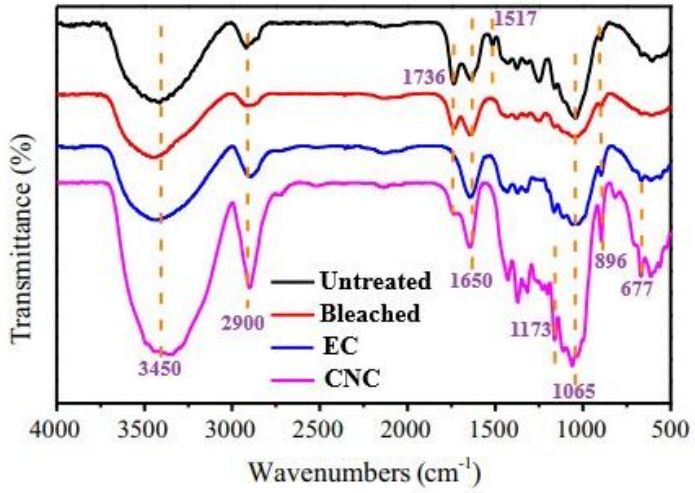

Fig. 4: FTIR Spectra of natural Pinus needles, bleached *Pinus* needles, extracted cellulose (EC) and crystalline nanocellulose (CNC)

In untreated pine needles, an intense peak at 1736 cm^{-1} appeared due to the existence of ester and acetyl functional groups in hemicellulose, also Ester bonds with the carboxylic acids of p-coumaric and ferulic acid present in lignin and hemicellulose (Dos Santos et al. 2013). The intensity of this peak lowers in every extraction step and it completely disappears for pure cellulose after exclusion of all amorphous lignin and hemicellulose regions. A weak intense characteristic peak of lignin at 1517 cm^{-1} is displayed in natural pine needles ascribed to C=C vibration(Neto et al. 2013).. After delignification, this peak also vanishes completely in the bleached product suggesting complete eradication of lignin. Due to strong H-bonding between water molecules and cellulose, a peak at 1650cm^{-1} for absorbed water molecules appears in all samples.

Two peaks at frequencies 1065 cm^{-1} and 896 cm^{-1} correspond to the C–O–C pyranose ring stretching vibration and C-H rocking vibration of regular cellulose (Haafiz et al. 2014). According to Dos Santos et al. (2013), the rise in these two peaks typically corresponds to an increase in cellulosic components. The resulting nanocellulose displayed high intense peak at 1065 and 896 cm^{-1} following alkali, bleaching, and acid hydrolysis treatments, suggesting a larger relative percentage of cellulose. In every wavenumber, the CNC's FTIR spectra resembled those of the extracted cellulose, indicating that the primary cellulose structures were not destroyed. Two further peaks at 1172cm-1 and 677cm-1 suggests the presence of SO_4^{2-} groups in CNC (Feng et al. 2015 and Morais et al. 2013). These findings demonstrate how well a multi-step treatment works to successfully remove non-cellulosic components while preserving cellulose structures. The crystallinity of CNC produced after hydrolysis and cellulose derived from pine needles were both analyzed using XRD tests. Figure 5 displays the XRD patterns for pine needles at various purification stages and CNC made following acid hydrolysis.

All of the diffractograms showed crystalline peaks and an amorphous broad hump, which are characteristics of semi-crystalline materials. Three distinct crystalline peaks were characteristic of cellulose I at around 2θ = 16º, 22.5º, and 35.2º. The (040), (002), and (101) lattice planes were identified as the sources of the experiential peaks at 2θ = 35.2°, 22.5º, and 16º respectively. These peaks were linked to the database with ID number COD 4114994 and belong to cellulose I (Wada et al. 2004). As anticipated, when cellulose was purified and amorphous lignin and hemicellulose were eliminated, the extents of these crystalline peaks rose (Fig. 5). The alkali-treated or bleached samples showed a widening of the diffraction peak at 2θ = 16º. The raw pine needles had a crystallinity index (CrI) of roughly 60.6, which is indicative of fibers from a secondary wall.

Alkali treatment raised the CrI value while bleaching treatment enhanced it even more. The percentages of CrI for biomass that was alkaline treated, and bleached, were found to be 68.3, and 72.6, respectively. These consequences imply that the crystallinity of the materials was affected by each stage of treatment. These results demonstrate that the treatment effectively eliminated the non-cellulosic amorphous polysaccharides. Under the circumstances employed in this investigation, it is anticipated that the cellulose's amorphous zones will be preferentially dissolved by the acid hydrolysis treatment. The hydronium ions successfully break down the glycosidic linkages hydrolytically, after entering the amorphous portions of cellulose resulting in the release of distinct crystallites. The increase in the CrI confirms that the major diffraction peak for CNC, which is positioned at 2θ = 22.5º, appears to be sharper and greater in amplitude, indicating more defined crystalline domains. The percentage of CrI for acid hydrolyzed biomass was found to be 82.7%.

Surface charge, size distribution and surface morphology: The SEM images of *Pinus* needles prior to and thereafter chemical treatment is shown in Fig 6. The raw pine needles are associated together by massive cementing material (hemicellulose and lignin) and appear as a rough rigid compact structure, but after alkali treatment, most of the hemicellulose and some part of the lignin gets dissolved in basic solution. Thus, in Fig 6b distinct cellulose fibers are visible.

Distinct cellulose fiber bundle in Fig. 6 (b) were because of hydrolysis of most of the hemicellulose and partial depolymerization of lignin. This finding implies that the structural elements of pinus needles were successfully eliminated by the alkaline treatment. The observation of individual cellulose fibres in Fig. 6(c) demonstrated the high efficacy of the

acidified sodium chlorite treatment in both lignin removal and cellulose fibre separation.

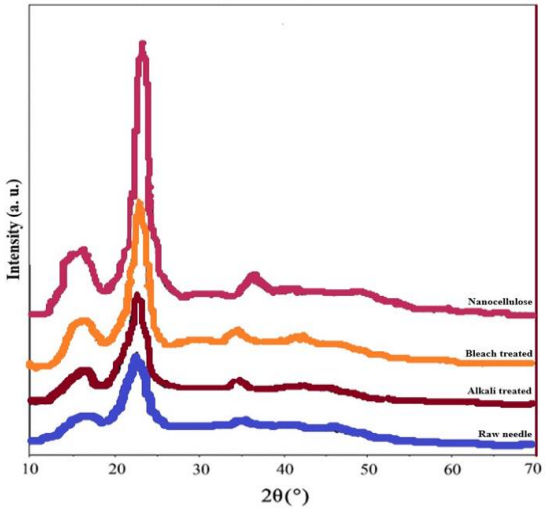

Fig. 5: XRD patterns of raw pine needles, alkali-treated biomass, bleach treated biomass and nanocellulose.

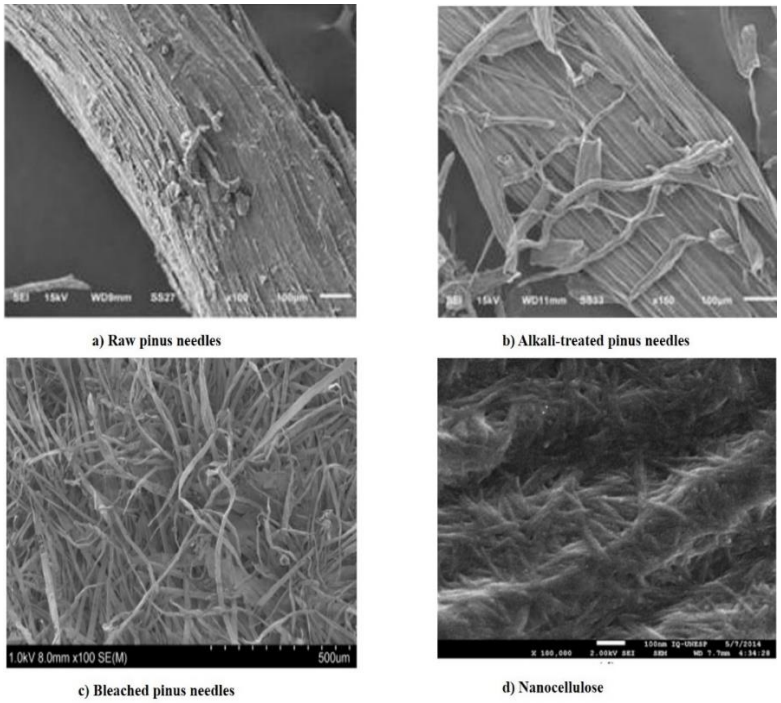

Fig. 6: SEM images of a) pine needles(raw) b) alkaline-treated raw needles c) bleached raw needle d) Nanocellulose

Moriana et al. (2016) found similar outcomes. They showed that the majority of the amorphous mechanisms are eliminated following the alkaline treatments, which opens the cell wall and release the cellulose fibers. However, a greater quantity of individualized fibers is produced as a result of the alkaline and bleaching treatments' increased removal of these compounds from the pine needles' cells. Fig. 6 (d) depicts the SEM image of nanocrystalline cellulose which has rod shaped morphology.

Furthermore, the isolation of nanoparticles with diameters and lengths of 13–20 nm and 149–250 nm, individually, was made possible by these hydrolysis conditions. Yu et al. (2012) also discovered that after acid hydrolysis the dimension of microcrystalline cellulose changed into rod shaped needle with length 200nm and diameter 20 nm.

Comparable findings were reported by other researchers for various biomass, including sugarcane bagasse (Verma et al. 2021) and rice husk (Johar et al. 2012).

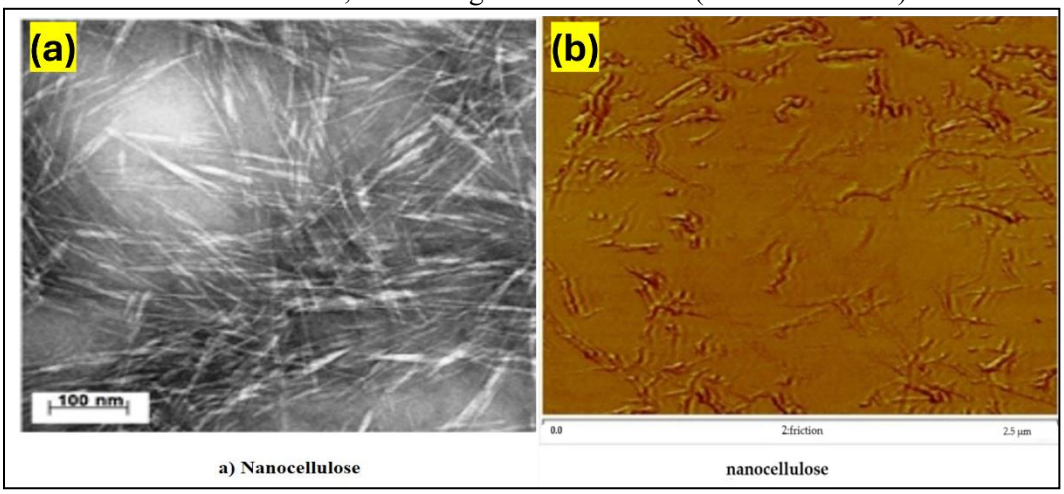

Fig. 7. (a) Transmission electron microscopy (TEM) images of nanocellulose (CNC), (b) AFM of nanocellulose crystal

The TEM images of cellulose nanocrystals in Fig. 7a illustrates the rod-like structure of CNCs having measurable length of 100-300nm and width 10-20nm. 2D AFM micrograph demonstrates that CNCs have an average length of 210 nm with an average diameter of 12nm (Fig. 7b). The CNCs developed from pine needles have a rod-like aspect and this data is in line with TEM and SEM analysis.

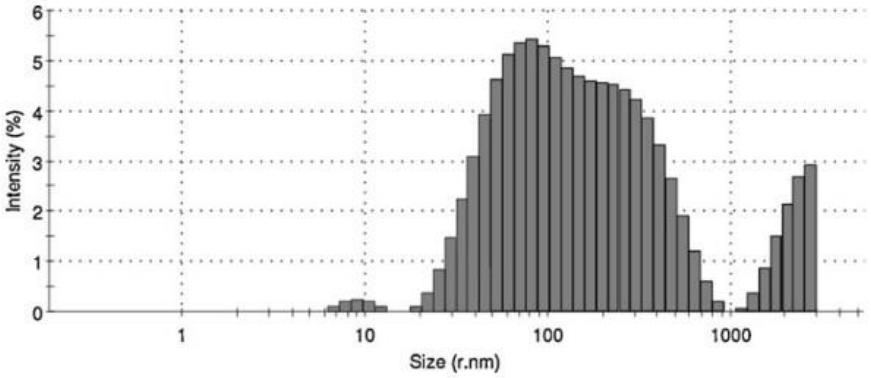

Fig. 8: Particle size distribution by DLS

In DLS analysis the particle size distribution resulted in three main groups: 0.8 % of the particles were around 9.19 nm, 87.6% were around 179.4 nm, and 11.6% were around 2.24 nm (Figure 8). The CNC particle size ranged between 140 and 530 nm, which is consistent with other studies of pinewood CNCs (Ditzel et al. 2017)

Thermal analysis

DSC thermograms of raw needles, pure cellulose, and nanocellulose shows two different endothermic processes. However, endotherms vary from one another and are highly characteristic of the material's composition (Mandal and Chakrabarty 2011). The first endotherm, which appears in all three situations at temperatures much below 100 °C, represents the moisture loss from evaporation. A good amount of heat was absorbed by raw pinus needle as compared to extracted cellulose and nanocellulose for losing the moisture, which is due to the presence of lignin, hemicellulose, and additional non-cellulosic constituents besides the cellulose itself. To maintain moisture in larger quantities, all of these hydrophilic compounds

also contribute to variations in the sorptive forces that hold this moisture in place. This may help to explain why moisture loss happens across a broad temperature range.

Since cellulose isolated from pinus needles lacks hemicellulose and lignin, it may have absorbed moisture with comparatively consistent sorptive pressures, resulting in moisture loss across a comparatively small temperature range. However, cellulose crystals in nanocellulose, especially those on their active surfaces, become sulfated, a process that significantly lowers the cellulose's affinity for absorbing moisture. As seen in Fig. 9, a little amount of moisture is adsorbed on its surfaces, but it is loosely bound and evaporates off at considerably lower temperatures, resulting in moisture loss across a narrow temperature range. In each of the three scenarios, the second endotherm provides insight into the melting process and the type of crystallite breakdown. When comparing raw pine needle to nanocellulose, the crystallinity increases. Because raw needle has a variety of constituents, each with a distinct melting range, we see the melting process take place over a broad temperature range, from 310 to 358 °C. After removal of most of the non-cellulosic components, crystalline cellulose was extracted. The narrow temperature range of (359.3– 363.7 °C) was observed for this crystalline cellulose due to its additional compressed crystal structure. After the elimination of amorphous regions by acid hydrolysis, nanocellulose crystals were isolated which often fuse to produce more compact and stiff structures. Therefore, CNC samples showed a further rise in sharpness and melting temperature (368.9–380.7 °C).

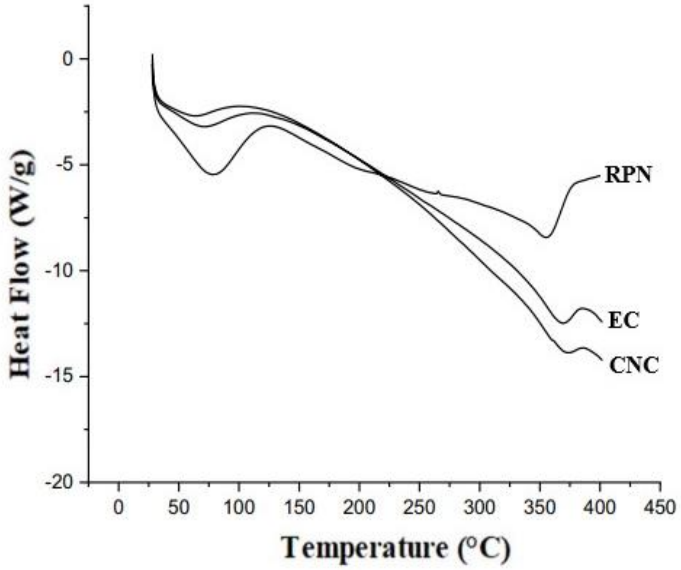

Fig. 9: DSC thermal transition curves of raw pine needle (RPN), extracted cellulose (EC) and nanocellulose (CNC)

Conclusion

Cellulose nanocrystals (CNC) were successfully extracted from *Pinus roxburghii* needles using eco-friendly techniques. Characterization through FTIR, XRD, SEM, TEM, AFM, DLS, and DSC confirmed their properties. XRD analysis showed increased crystallinity due to the removal of amorphous components. TEM, AFM, and SEM revealed a rod-like morphology with dimensions of 100–300 nm in length and 10–20 nm in width. DSC analysis indicated superior thermal stability compared to raw biomass. These CNCs are biodegradable, biocompatible, and regenerative biopolymers with vast

nanotechnological applications, making them valuable for sustainable material development.

Acknowledgement

All the authors acknowledge IIT Roorkee, IIT Ropar, USIC H.N.B. Garhwal University, Srinagar, and UGC-SAIF, DST-FIST Department of Chemistry, H.N.B. Garhwal University, Srinagar for helping with the characterization of all the synthesized samples.

References

Azizi S, Ahmad MB, Ibrahim NA, Hussein MZ, Namvar F. (2014) Cellulose nanocrystals/ZnO as a bifunctional reinforcing nanocomposite for poly (vinyl alcohol)/chitosan blend films: fabrication, characterization and properties. *International journal of molecular sciences.* 15(6):11040-53.

Babick F. (2020) Dynamic light scattering (DLS). In: Characterization of nanoparticles, Elsevier. 137-172.

Balakrishnan P, Geethamma VG, Sreekala MS, Thomas S. (2018) Polymeric biomaterials: State-of-the-art and new challenges. In Fundamental biomaterials: polymers. Woodhead Publishing, pp. 1-20.

Costa LA, Fonseca AF, Pereira FV, Druzian JI. (2015) Extraction and characterization of cellulose nanocrystals from corn stover. *Cellulose Chemistry and Technology*. 49(2):127-33.

De Blasio C. (2019) Thermogravimetric analysis (TGA). Fundamentals of Biofuels Engineering and Technology. 91-102.

De Souza Lima, M. M., & Borsali, R. (2004). Rodlike cellulose microcrystals: Structure, properties, and applications. *Macromolecular Rapid Communications*, *25*(7), 771–787. https://doi.org/10.1002/marc.200300268

Ditzel FI, Prestes E, Carvalho BM, Demiate IM, Pinheiro LA. (2017) Nanocrystalline cellulose extracted from pine wood and corncob. *Carbohydrate Polymers.* 157:1577-85.

Dos Santos RM, Neto WP, Silvério HA, Martins DF, Dantas NO, Pasquini D. (2013) Cellulose nanocrystals from pineapple leaf, a new approach for the reuse of this agro-waste. *Industrial Crops and Products*. 50:707-14.

Fardioui M, Stambouli A, Gueddira T, Dahrouch A, Qaiss AEK, Bouhfid, R. (2016). Extraction and characterization of nanocrystalline cellulose from doum (*Chamaerops humilis*) leaves: a potential reinforcing biomaterial. *Journal of Polymers and the Environment*. 24: 356-362.

Feng X, Meng X, Zhao J, Miao M, Shi L, Zhang S, Fang J. (2015) Extraction and preparation of cellulose nanocrystals from dealginate kelp residue: structures and morphological characterization. *Cellulose*. 22:1763-72.

Gibril M E, Ahmed K, Lekha P, Sithole B, Khosla A, Furukawa H. (2022) Effect of nanocrystalline cellulose and zinc oxide hybrid organic–inorganic nanofiller on the physical properties of polycaprolactone nanocomposite films. *Microsystem Technologies*. 28(1):143-52.

Haafiz MM, Hassan A, Zakaria Z, Inuwa IM. (2014) Isolation and characterization of cellulose nanowhiskers from oil palm biomass microcrystalline cellulose. *Carbohydrate polymers*.103:119-25.

Johar N, Ahmad I, Dufresne A. (2012) Extraction, preparation and characterization of cellulose fibres and nanocrystals from rice husk. *Industrial Crops and Products*. 37(1):93-9.

Kala LD, Subbarao PM. (2018) Estimation of pine needle availability in the Central Himalayan state of Uttarakhand, India for use as energy feedstock. *Renewable Energy.* 128:9-19.

Kalia S, Dufresne A, Cherian BM, Kaith BS, Avérous L, Njuguna J, Nassiopoulos E. (2011) Cellulose-based bio-and nanocomposites: a review. *International journal of polymer science*. 2011(1):837875.

Khalil H A, Davoudpour Y, Islam M N, Mustapha A, Sudesh K, Dungani R, Jawaid M. (2014). Production and modification of nanofibrillated cellulose using various mechanical processes: a review. *Carbohydrate polymers*. 99:649-65.

Klemm D, Heublein B, Fink H & Bohn A (2005). Cellulose: Fascinating Biopolymer and Sustainable Raw Material. *Angewandte Chemie International Edition*, *44*(22), 3358–3393. https://doi.org/10.1002/anie.200460587

Kumar A, Negi YS, Choudhary V, Bhardwaj NK. (2014) Characterization of cellulose nanocrystals produced by acid-hydrolysis from sugarcane bagasse as agro-waste. *Journal of Materials Physics and Chemistry*. 2(1):1-8.

Leyva-Porras C, Cruz-Alcantar P, Espinosa-Solís V, Martínez-Guerra E, Piñón-Balderrama CI, Compean Martínez I, Saavedra-Leos MZ. (2019) Application of differential scanning calorimetry (DSC) and modulated differential scanning calorimetry (MDSC) in food and drug industries. *Polymers*. 12(1):5.

Lee K-Y, Buldum G, Mantalaris A & Bismarck A (2014). More Than Meets the Eye in Bacterial Cellulose: Biosynthesis, Bioprocessing, and Applications in Advanced Fiber Composites: More Than Meets the Eye in Bacterial Cellulose: Biosynthesis, Bioprocessing …. *Macromolecular Bioscience*, 14(1), 10–32. https://doi.org/10.1002/mabi.201300298

Mandal A, Chakrabarty D. (2011) Isolation of nanocellulose from waste sugarcane bagasse (SCB) and its characterization. *Carbohydrates Polymers*. 86, 1291-1299.

Michelin M, Gomes D G, Romaní A, Polizeli M D L T M & Teixeira J A (2020). Nanocellulose Production: Exploring the Enzymatic Route and Residues of Pulp and Paper Industry. *Molecules*, *25*(15), 3411. https://doi.org/10.3390/molecules25153411

Moriana R, Vilaplana F, Ek M. (2016) Cellulose nanocrystals from forest residues as reinforcing agents for composites: a study from macro-to nano-dimensions. *Carbohydrate polymers*. 139:139-49.

Nam S, French AD, Condon BD, Concha M. (2016) Segal crystallinity index revisited by the simulation of X-ray diffraction patterns of cotton cellulose Iβ and cellulose II. *Carbohydrate polymers*. 135:1-9.

Nasir M, Hashim R, Sulaiman O & Asim M (2017). Nanocellulose. In *Cellulose-Reinforced Nanofibre Composites* (pp. 261–276). Elsevier. https://doi.org/10.1016/B978-0-08-100957-4.00011-5

Neto WPF, Silvério HA, Dantas NO, Pasquini D (2013). Extraction and characterization of cellulose nanocrystals from agro-industrial residue–Soy hulls. *Industrial Crops and Products*. 42:480-8.

Ng HM, Sin LT, Tee TT, Bee ST, Hui D, Low CY, Rahmat AR. (2015) Extraction of cellulose nanocrystals from plant sources for application as reinforcing agent in polymers. Composites Part B: *Engineering*. 75:176-200.

Rambabu N, PAnthapulakkal S, Sain M, Dalai AK. (2016). Production of nanocellulose fibers from pinecone biomass: Evaluation and optimization of chemical and mechanical treatment conditions on mechanical properties of nanocellulose

films. *Industrial Crops and Products*. 83:746-54.

Thakur VK, Singha AS, Thakur MK. (2013) Fabrication and physico-chemical properties of high-performance pine needles/green polymer composites. *International Journal of Polymeric Materials and Polymeric Biomaterials.* 62(4):226-30.

Thakur V, Guleria A, Kumar S, Sharma S & Singh K (2021). Recent advances in nanocellulose processing, functionalization and applications: A review. *Materials Advances*, *2*(6), 1872–1895. https://doi.org/10.1039/D1MA00049G

Verma C, Chhajed M, Gupta P, Roy S, Maji PK. (2021) Isolation of cellulose nanocrystals from different waste bio-mass collating their liquid crystal ordering with morphological exploration. *International Journal of Biological Macromolecules*. 175:242-53.

Wada M, Heux L, Sugiyama J. (2004) Polymorphism of cellulose I family: reinvestigation of cellulose IVI. Biomacromolecules. 5(4):1385-91.

Lin N & Dufresne A (2014). Nanocellulose in biomedicine: Current status and future prospect. *European Polymer Journal*, *59*, 302–325. https://doi.org/10.1016/j.eurpolymj.2014.07.025

Yadav S K (2016). *Nanoscale Materials in Targeted Drug Delivery, Theragnosis and Tissue Regeneration*. Springer Singapore. https://doi.org/10.1007/978-981-10-0818-4

Yu HY, Qin ZY, Liu YN, Chen L, Liu N, Zhou Z (2012) Simultaneous improvement of mechanical properties and thermal stability of bacterial polyester by cellulose nanocrystals. *Carbohydrate polymers*. 89(3):971-8.